Optical-absorption coefficient measurements in solids and liquids using correlation photoacoustic spectroscopy

JAMES T. DODGSON, ANDREAS MANDELIS, AND CLAUDIO ANDREETTA
Photoacoustic and Photothermal Sciences Laboratory, Department of Mechanical Engineering, University of Toronto, Toronto, Ont., Canada M5S 1A4

Received August 8, 1985

The spectroscopic information related to the optical-absorption coefficients of solids and liquids, which is contained in the signal-magnitude and time-delay channels of cross-correlation photoacoustic spectroscopy (CPAS), has been investigated. Powders of holmium oxide and aqueous solutions of black India ink of variable concentrations were used as solid and liquid samples, respectively. The experimental results were found to be in general agreement with a one-dimensional theoretical model of the CPAS-signal generation.

On a étudié l'information spectroscopique relative au coefficient d'absorption optique des solides et liquides, qui est contenue dans les modes amplitude du signal et temps de délai de la technique de spectroscopie photo-acoustique à corrélation croisée (CPAS). Des poudres d'oxyde de holmium et des solutions aqueuses d'encre de Chine noire de concentrations variables ont été utilisées comme échantillons solides et liquides respectivement. Les résultats expérimentaux ont été trouvés en accord général avec le modèle théorique unidimensionnel de la génération du signal dans la technique CPAS.

[Traduit par la revue]

Can. J. Phys. **64**, 1074 (1986)

1. Introduction

Correlation photoacoustic spectroscopy (CPAS) is a relatively new technique, first reported in 1980 by Kato *et al.* (1). In that work and subsequent publications (2, 3), the main emphasis has been given to establishing the potential of CPAS as a technique capable of performing depth-profiling and thermal-wave imaging in layered solids in a qualitative fashion. The spectroscopic abilities of CPAS have also been investigated qualitatively, simultaneously with its depth-profiling character (1, 2, 4, 5). CPAS has thus been shown to be capable of producing spectra of solids when the wavelength of the exciting radiation is scanned.

The spectroscopic character of CPAS has not yet been investigated systematically and (or) quantitatively. The experimentally obtained photoacoustic spectra, however, are expected to be subject to limitations such as photoacoustic saturation (6) and microphone-frequency response (7). Sugitani *et al.* (2) have shown that the cross-correlation function of the input and the resultant output function of a randomly excited linear system is equal to the impulse-response function of the system. It is, therefore, expected that the equivalent-pulse duration of a pseudorandom Binary Sequence (PRBS) optical excitation will affect the cross-correlation PAS response of the system in both magnitude and time delay (8).

In this paper we present a spectroscopic investigation of the optical-absorption coefficient dependence of CPAS in solids and liquids. The experimental results are compared with numerical data from a proposed theoretical model. We are thus able to determine the conditions under which CPAS can be used as a quantitative spectroscopic technique, capable of measuring optical-absorption coefficients in the solid and liquid states.

2. Instrumentation and materials

A schematic diagram of the experimental apparatus is shown in Fig. 1. Light sources used for optical excitation of the samples were a 1-mW He–Ne laser, or the light from a 1000-W Xe lamp (Oriel model 6141 with photofeedback control) monochromatized by use of an Instruments SA, Model H-20 holographic-grating monochromator. For CPAS measurements, a special light chopper was made based on a pseudorandom binary sequence, similar to the one used by Sugitani *et al.* (2). The chopper blade, machined out of a 1/16-in. black anodized aluminum plate, was fitted to the chopper blade holder of an AMKO model OC 4000 mechanical chopper (1 in. = 2.54 cm). This allowed control of the rotation frequency of the PRBS chopper via calibration of the motor-driven digital display through a light-emitting diode located at the base of the chopper blade holder. The quartz beam splitter was used to direct a fraction of the radiation to the UV-enhanced photodiode (Silicon Detector Corp. model SD-100-13-13-022), whose signal, when amplified by a Keithley model 427 current amplifier, was used as the sample-exciting optical wave train. The output of the photoacoustic cell, EG & G Princeton Applied Research model 6003 and matching preamplifier model 6005, was further filtered through passage from an Ithaco model 1201 low-noise preamplifier – band-pass filter. A DEC PDP11/23 computer was interfaced to the experimental setup with the aid of a Data Translation analog–digital converter (model DT 3392). This is a 12-bit converter operational at frequencies up to 125 kHz for two channels. Cross correlations were performed digitally.

The materials used for spectroscopic investigations were Ho_2O_3 powder (Aldrich Chemical Co., 99.9% purity) and aqueous solutions of black India ink (REGAL India Ink, L. A. Reeves Ink Co. Ltd., Downsview, Ont.). The rare-earth oxide was chosen for the strong and sharp transition peaks it exhibits in its visible absorption spectrum, which is a means of variation of the absorption coefficient (9); it was also used in a powdered form owing to the high surface-to-volume ratio of the particulates, which enhanced the CPAS signal-to-noise ratio (SNR) considerably. The spectral region chosen for Ho_2O_3 CPAS was between 420 and 515 nm, as the Ho^{3+} ion exhibits a strong, broad absorption band for the 8-nm resolution of our experiments. This broad band, in fact, consists of spectral peaks given the assignations $^5F_2$ (474 nm), $^3K_8$ (464 nm), $^5G_6$ (457 nm), and $^5G_5$ (450 nm). Of the four peaks, all resolvable with our apparatus at 2-nm resolution, the first peak appears as a broad shoulder and the last three are broadened to form the observed broad band at the 8-nm resolution level.

Samples were also prepared using the India ink in aqueous solutions of 100, 75, 50, 25, 20, 15, and 10% ink by volume. The solutions were subsequently sealed in vials, until they were used, to ensure minimum water evaporation.

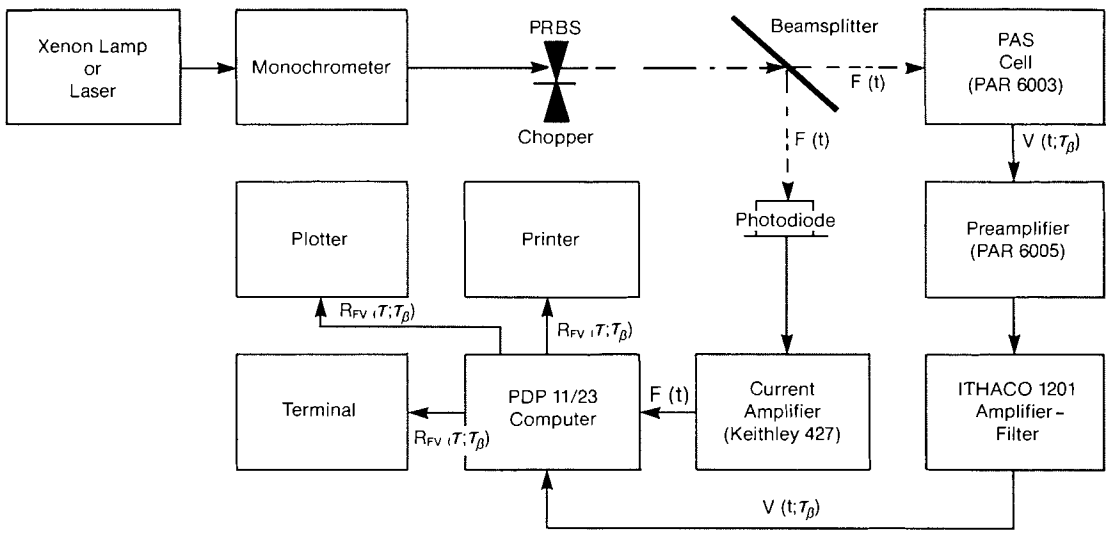

FIG. 1. The CPAS microphone–gas coupled experimental apparatus.

3. Experimental and results

For reasons of comparison between experiment and CPAS theory (10), the thermal-diffusivity and optical-absorption spectra of Ho_2O_3 were measured using a conventional frequency-domain photoacoustic (F-D PAS) spectrometer described elsewhere (11). To use the well-known method of thermal-diffusivity calculation from the slope of the PAS phase vs. frequency curve (12), a thin layer of Ho_2O_3 powder (39 ± 10 μm) was deposited on a carbon-black backing and irradiated with 515-nm light, i.e., in a spectral region where the optical-absorption coefficient has a minimum (9). In this manner, the Ho_2O_3 thin layer was expected (and later proven) to be optically transparent ($\beta l \cong 2 \times 10^{-3}$). Transparency was verified by examining two PAS spectra spanning the 420- to 520-nm region at 50 and 100 Hz. Comparison of the ratio R_p of the two peak signals at 450 nm and that of the two valleys, R_v, at 515 showed that the valley signals contained a strong component from the underlying carbon black,

$$R_p(50\,\text{Hz}/100\,\text{Hz}) = 2.2 < R_v(50\,\text{Hz}/100\,\text{Hz}) = 4.67$$

Figure 2 shows the F-D PAS phase data obtained from the Ho_2O_3 thin layer for 515-nm illumination at chopping frequencies between f = 50 and 200 Hz. Phase differences $\Delta\psi$ were measured with the sample in place and with an empty holder. The thermal diffusivity of Ho_2O_3 was calculated, assuming the powder to be transparent and using the equation (13, 14)

$$[1] \quad \Delta\psi = [(\pi/\alpha_s)^{1/2} l]\sqrt{f}$$

A least squares fit to the data in Fig. 2 gave a slope value from which the thermal diffusivity was found to be

$$[2] \quad \alpha_{Ho_2O_3} = 0.0059 \pm 0.0004\,\text{cm}^2/\text{s}$$

To our knowledge, this is the first calculation of the thermal diffusivity of Ho_2O_3. Comparisons can be made, however, to other rare-earth oxides. The literature values for yttrium oxide (Y_2O_3), samarium oxide (Sm_2O_3), erbium oxide (Er_2O_3), and lutetium oxide (Lu_2O_3) are (15), respectively, 0.015, 0.0049, 0.012, and 0.014 cm^2/s at 20°C. The determined value for Ho_2O_3 certainly fits into this range and is subsequently used in our theoretical calculations. The reproducibility of the results and general reliability of the frequency-scanning method for the determination of powder thermal diffusivities appears to be very good, provided the layers are thermally and optically thin.

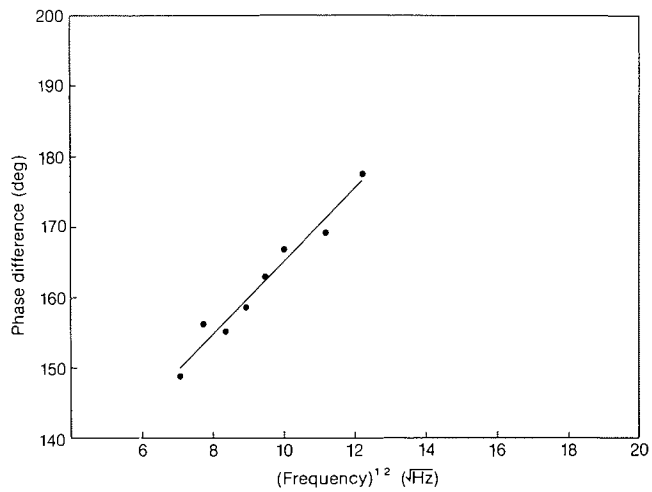

FIG. 2. Least squares fit to the F-D PAS phase lag vs. square root of modulation frequency for 39 ± 10-μm-thick Ho_2O_3 powders on black backing. Irradiation wavelength = 515 nm.

The values for the optical-absorption coefficient have been determined by normalizing the F-D PAS holmium oxide spectrum to a single value for β (446 nm), calculated from recent work by Carlson and Hodul (16). From that study, the value of β at 446 nm is found to be 22.44 cm^{-1} with 2-nm resolution. The normalized optical-absorption spectrum of Ho_2O_3 powder in this work (8-nm resolution) is shown in Fig. 3.

The CPAS spectrum of holmium oxide powder is shown in Fig. 4 with the delay time as a parameter. The spectrum has been normalized by the Xe-lamp spectral throughout, using Xerox toner as a black absorber. The three-dimensional surface shows the expected strong absorption between 445 and 470 nm flanked by relatively transparent regions. In the strongly absorbing region and behind the frontal peaks, a depression mirroring the peak intensities can be seen. We believe this depression to be due to the microphone "flyback" effect, which has been observed in the impulse-response studies of Cox and Coleman (17). These authors have found that in impulse-response PAS, the signal depression below the baseline noise level after the end of the optical pulse is due to the microphone

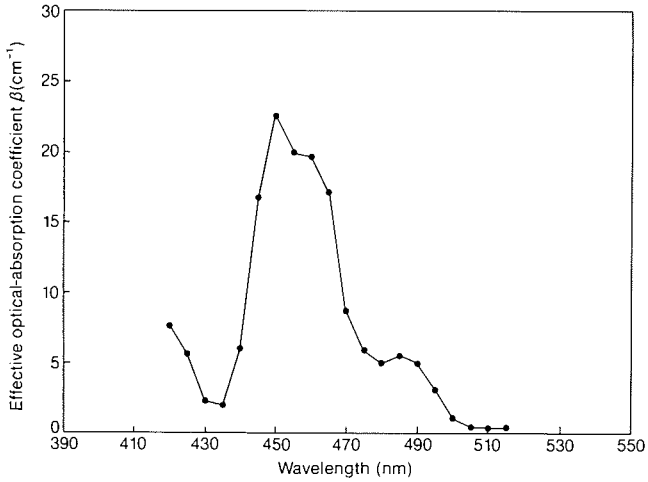

FIG. 3. Effective optical-absorption spectrum of Ho_2O_3 powders determined photoacoustically with 8-nm resolution, using data from Carlson and Hodul (15).

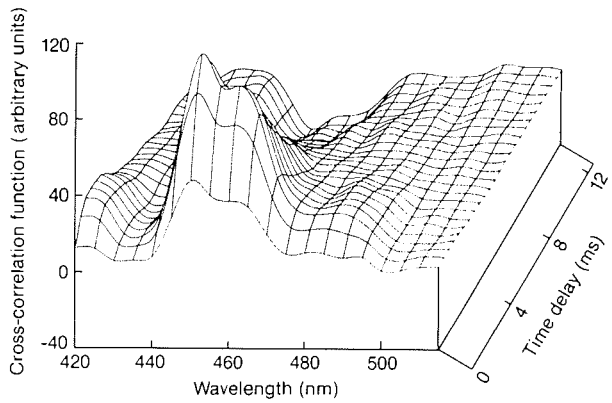

FIG. 4. Cross-correlation function (CPAS spectrum) of the normalized signal from Ho_2O_3 powder. Chopper speed = 6 rps; preamp filter band pass = 30 Hz–10 kHz.

overshooting the actual pressure in the cell because of the rapid change in pressure with strongly absorbing samples. This effect can ultimately be traced to the mechanical inertia of the microphone diaphragm itself.

The cross-correlation function

$$[3] \quad R_{FV}(\tau;\tau_\beta) = \lim_{T\to\infty} \frac{1}{2T} \int_{-T}^{T} F(t)V(t+\tau;\tau_\beta)\,dt$$

for Ho_2O_3 at various absorption-coefficient values between 436 and 450 nm is shown in Fig. 5. Most of the parameters in [3] have been defined in Fig. 1. Briefly, $F(t)$ is the sample-exciting pseudorandom optical wave form; $V(t;\tau_\beta)$ is the photoacoustic response of the sample; $\tau_\beta \equiv (\beta^2\alpha_s)^{-1}$ is a material-characteristic parameter (8, 10) corresponding to the thermal transit time to the sample surface from a depth equal to the wavelength-dependent optical-absorption length, $\mu_\beta = [\beta(\lambda)]^{-1}$; and T is the pseudoperiod. In the spectral region of Fig. 5, the powder changes from optically transparent to opaque. With the value for $\alpha_{Ho_2O_3}$ given by [2] and a sample thickness of ca. 1.6 mm, the sample is found to be thermally thick at all times during a cross-correlation experiment; the thermal transit time through the sample thickness is calculated to be 4.12 s, much greater than the longest light-pulse duration of 9.2 ms. In Fig. 5 the CPAS magnitude decreases with decreasing β.

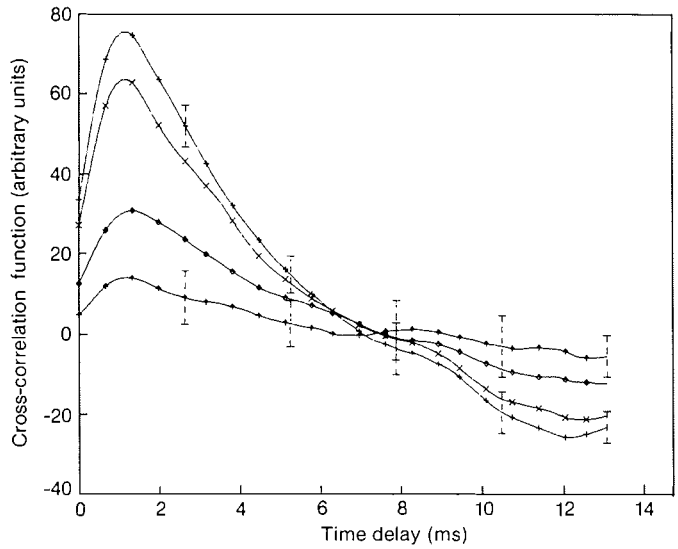

FIG. 5. Cross-correlation function of Ho_2O_3 at various wavelengths (nm): +, 450 ($\beta \cong 22.4\,cm^{-1}$); ×, 446 ($\beta \cong 16.6\,cm^{-1}$); ◆, 442 ($\beta \cong 6.5\,cm^{-1}$); ↑, 438 ($\beta \cong 5.5\,cm^{-1}$).

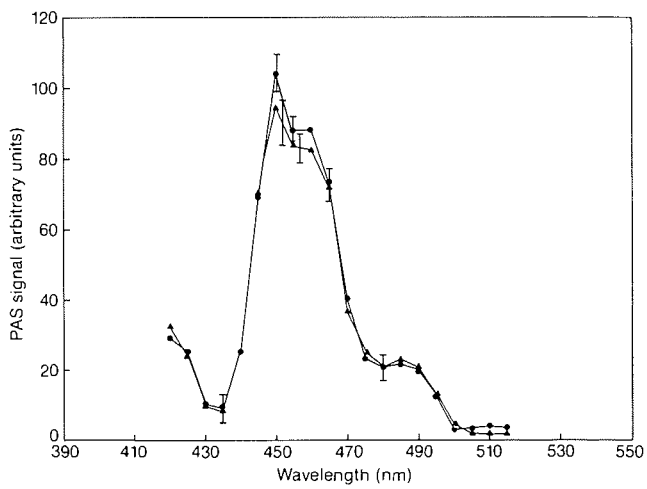

FIG. 6. The F-D PAS (▲) amplitude at 50 Hz and CPAS (●) magnitude at 6 rps. Both curves were artificially matched at 440 nm.

Figure 6 shows a comparison between a normalized F-D PAS spectrum of Ho_2O_3 (photoacoustic amplitude) taken with lock-in detection at 50 Hz and the normalized CPAS average magnitude of 20 cross correlations, at the peak time delay taken at 6 rps. The detailed agreement of the spectral features across the transition band confirms that the peak magnitude of the CPAS gives optical-absorption information equivalent to the conventional F-D PAS. The difference between the two signals at high values of β may be due to different onsets of photoacoustic saturation for the two methods. This point is discussed further below.

The sample holder used for the determination of the optical-absorption coefficients of the aqueous ink solutions consisted of two microscope slides separated by a single layer of aluminum foil 20 ± 1 μm thick, used as a spacer. The foil had an opening in its center into which the liquid was injected with care so as not to leave air gaps or create air bubbles. The average sample thickness used in this work was thus found to be 20.25 μm. The experimental configuration consisted of the He–Ne laser irradiating the sample vertically with intermittent

TABLE 1. Optical-absorption coefficients of aqueous solutions of India ink determined via transmission measurements

Ink concentration (% vol.)	β^a (cm^{-1})	$\mu_\beta{}^b$ (μm)
100	1785.7 ± 52.9	5.6
75	618.5 ± 28.6	16.2
50	365.3 ± 32.8	27.4
25	114.2 ± 10.6	87.6
20	87.0 ± 3.2	114.9
15	59.9 ± 9.7	166.9
10	17.1 ± 9.9	584.8

[a] $\beta = (1/L) \ln (V_0/V_t)$; L, liquid thickness; V_0, incident light intensity in volts (lock-in signal amplitude); V_t, transmitted intensity.
[b] $\mu_\beta \equiv 1/\beta$.

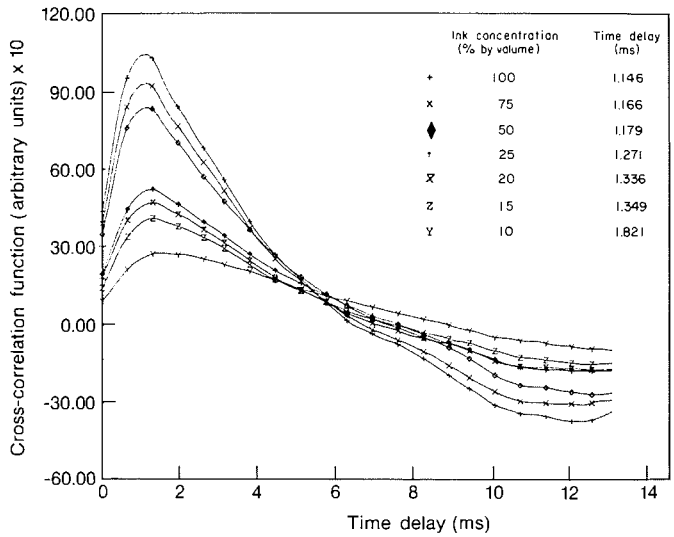

FIG. 7. The CPAS magnitude of aqueous ink solutions. Chopper speed = 6 rps.

light at 100 Hz, and the Silicon Detector Corp. photodiode receiving the focussed light transmitted through a solution of predetermined concentration. Lock-in detection and use of the Beer–Lambert law yielded values for the optical-absorption coefficients, shown in Table 1. After the optical measurements, liquid samples of the same solutions were placed in the PAS cell. With the value for the sample's thermal diffusivity assumed to be that of water, $\alpha_s = 1.4 \times 10^{-3}\,cm^2/s$ (18), all samples were calculated to be thermally thick at all times during the cross-correlation experiments (thermal transit time = 18.3 s).

Figure 7 shows CPAS results obtained from all the prepared solutions, using the same computer methods as for Ho_2O_3. Cross correlations obtained from ink solutions weaker than 10% by volume suffer from poor SNR and are not considered further in this work. The negative values of the correlations are attributed to the microphone flyback effect.

4. Discussion

The optical-absorption coefficient values calculated (10) for Ho_2O_3 (Fig. 3) and measured for the ink solutions (Table 1) spanned two and three orders of magnitude, respectively, and thus provided a broad range for testing the spectroscopic capabilities of CPAS. For interpretation purposes, it would have been more desirable to use single-crystalline materials for the solid-state experiments, which could be assumed to be truly one-dimensional with respect to their optical and thermal properties. Preliminary tests with CdS single crystals, unfortunately, exhibited SNRs too low for the quantitative purposes of the present work, even at super-bandgap excitations. Spectroscopic data of hydrated Ho_2O_3 pastes showed no difference from the powdered samples, and subsequently the powders were treated as one-dimensional samples.

The experimental CPAS data have been compared with predictions from a proposed theoretical model (10). According to that model, the microphone-voltage signal is generated owing to the photoacoustic response of an absorbing material, which is optically excited by a pseudorandom input

$$[4]\quad F(t) = \sum_{j=1}^{N} f_j(t)$$

$$f_j(t) = \begin{cases} 1; & \tau_{j-1} < t < \tau_j \\ 0; & \tau_j < t < \tau_{j+1} \end{cases}$$

where N square optical pulses were assumed, the duration of the jth pulse being variable and given by

$$[5]\quad \Delta\tau_j = \tau_{2j-1} - \tau_{2j-2}$$

The microphone response to the PRBS excitation, [4], was found to be

$$[6]\quad V(t;\tau_\beta) \cong GY(\beta)\tau_\beta \begin{cases} \sum_{j=1}^{N-1} \{Z[(t-\tau_{2j-1})/\tau_\beta] - Z[(t-\tau_{2j-2})/\tau_\beta]\} + Z(0) - Z[(t-\tau_{2N-2})/\tau_\beta]; & \tau_{2N-2} \le t \le \tau_{2N-1} \\ \sum_{j=1}^{N} \{Z[(t-\tau_{2j-1})/\tau_\beta] - Z[(t-\tau_{2j-2})/\tau_\beta]\}; & t \ge \tau_{2N-1} \end{cases}$$

where G is a constant dependent on microphone parameters,

$$[7]\quad Z(x) \equiv e^x \operatorname{erfc}(\sqrt{x})$$

with

$$[8]\quad \sum_{j=1}^{N-1} \{\,\} = 0, \qquad N = 1$$

and

$$[9]\quad Y(\beta) \equiv P_0 I_0 \eta \beta \alpha_g^{1/2}/T_0 L k_s, \qquad \text{see ref. 6}$$

Utilizing the values for $\alpha_{Ho_2O_3}$ and $\beta_{Ho_2O_3}(\lambda)$ found in our experiments, as well as those for the ink solutions, we calculated the cross-correlation function for a particular $F(t)$ input given by [4] and an output $V(t;\tau_\beta)$ predicted from [6]. To model our experiments as closely as possible, the PRBS sequence that was used in the experiments was also modeled as $F(t)$ in the theoretical analysis. The PRBS was broken down into 1270 discrete time intervals, just as in the experiments, and the resulting theoretical microphone response was cross correlated numerically with the PRBS optical-excitation wave train. Each

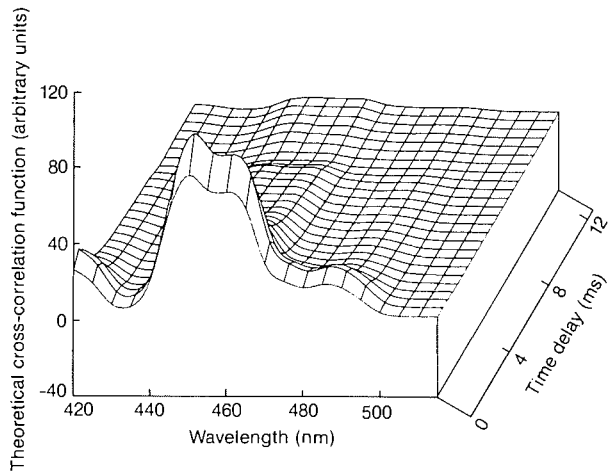

FIG. 8. Theoretical cross-correlation function (CPAS spectrum) of the normalized signal from the Ho_2O_3 powder. Chopper speed = 6 rps.

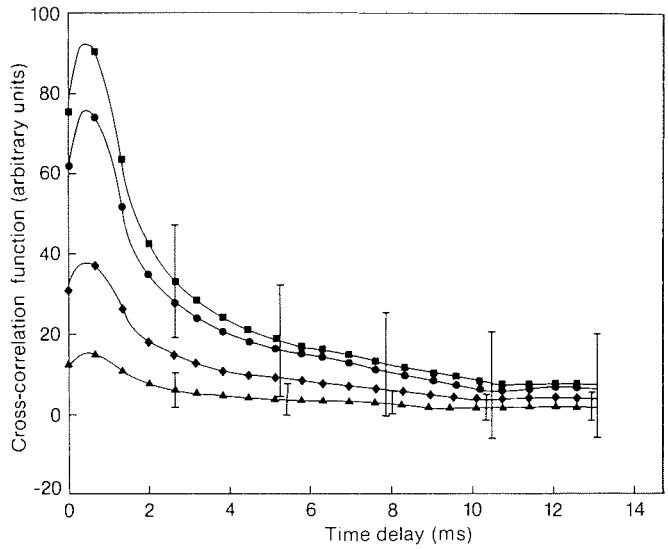

FIG. 9. Theoretical cross-correlation function of Ho_2O_3 at various wavelengths (nm): ■, 450; ●, 446; ◆, 442; ▲, 438.

series of calculations was made equal in duration to one rotation of the chopper blade, and each series was repeated 20 times at different starting positions of the wave train to model the different starting positions that occurred in the experiments. From this procedure, the mean and standard deviations of the cross-correlation function and of the peak time delay were determined.

Using the experimentally determined α_s and $\beta(\lambda)$ values, we first apply the theory to Ho_2O_3. The results of the theory are illustrated in Figs. 8 and 9. Comparison of Figs. 8 and 4 indicates that the theory predicts the experimental results well except for the flyback microphone effect and the absolute value of the peak time delay. Figure 9 is also in general qualitative agreement with Fig. 5. The apparent discrepancy in the values of peak delay times between these two figures is believed to be caused by the roll-off in the microphone-frequency response above 10 kHz, which coincides with the earliest measurable cross-correlation times τ in our experiments. The microphone flyback effect, which is assumed to cause the crossing of the curve in Fig. 5, is also absent from Fig. 9.

Figure 10 shows a comparison between the CPAS peak magnitude obtained from Ho_2O_3 experimentally at 8-nm resolution and that obtained using [6] with the calculated values of α_s and $\beta(\lambda)$. The agreement is very good except for the highest β values and indicates that the theory presented here can adequately describe the spectroscopic capabilities of CPAS. The departure of the theoretical curve from the data points at high values of β has been attributed to the difference between the values of β used in the model in this spectral region and the actual β values, which our 8-nm-resolution spectrometer could not accurately measure.

Within the optical-absorption coefficient range of the investigated Ho_2O_3 absorption band, the relationship between $\beta(\lambda)$ and the experimental and theoretical peak magnitudes of the CPAS signal is found to be linear, see Fig. 11. The agreement in both absolute values of the cross-correlation functions and slopes is very good. Figure 11 shows that CPAS is a sensitive spectroscopic technique in the range of β values involved and can be used quantitatively with the presented theory, [4]–[9], to predict absolute values of β. The linear dependence of CPAS magnitude on β is because for the β values employed, the photoacoustic signal is far from saturation and can be shown (6) to be proportional to β.

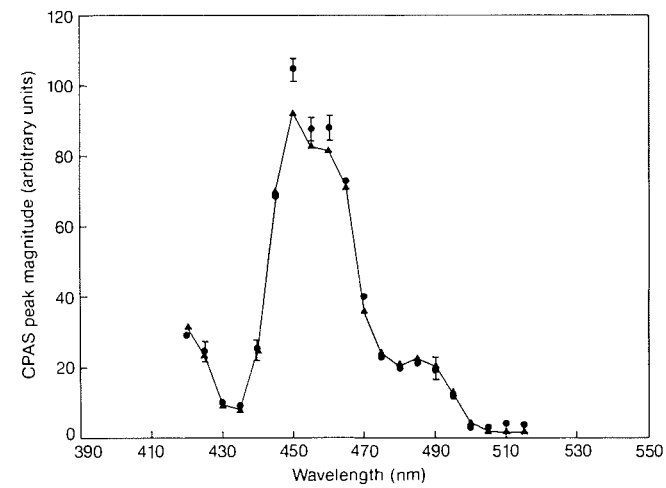

FIG. 10. Wavelength dependence of the CPAS magnitude of Ho_2O_3 at the peak delay time: ●, experimental; ▲, theoretical.

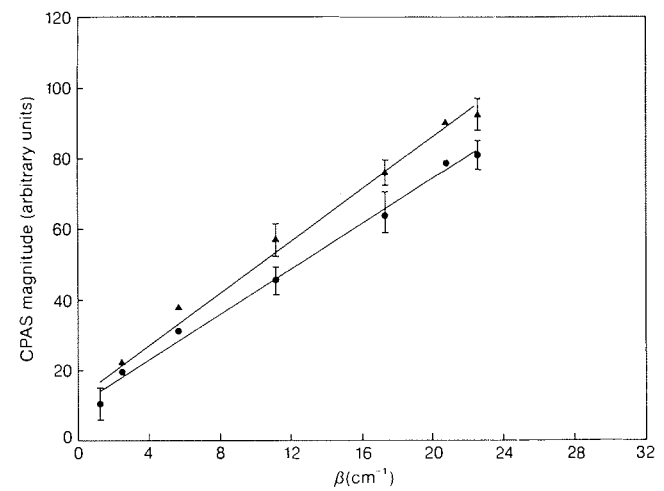

FIG. 11. The CPAS magnitude vs. optical-absorption coefficient for Ho_2O_3: ●, experimental; ▲, theoretical.

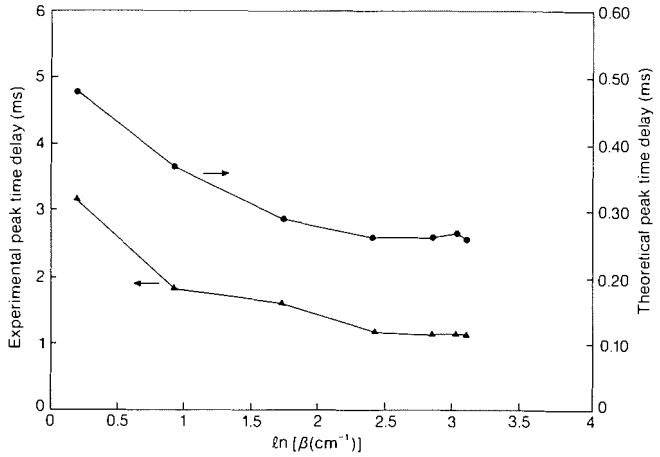

FIG. 12. The CPAS peak delay-time variation with the optical-absorption coefficient for Ho_2O_3: ●, experimental; ▲, theoretical.

The CPAS peak time delay, τ_0, does not have a simple relationship to β, either experimentally or theoretically. In general, τ_0 increases as β decreases. The variation of τ_0 with the natural logarithm of β for the experimental and theoretical results can be seen in Fig. 12. In this figure the absolute-value discrepancy between the theoretical and experimental values is apparent, as discussed above; however, the trends with β are similar in both curves.

Figure 13 shows the CPAS peak magnitude (*a*) and time delay (*b*) as a function of β for the ink solutions. In this case, the range of optical-absorption coefficients is broader than those calculated for Ho_2O_3. The magnitude curve exhibits photoacoustic saturation at high values of β and an essentially linear dependence of the CPAS signal on β at low values of this parameter, in agreement with the Rosencwaig–Gersho theory (6). This linear behavior is also consistent with the spectroscopic data of Fig. 11 for Ho_2O_3 at low values of the absorption coefficient. The onset of saturation at ca. $\beta \cong 500\,cm^{-1}$ is in the same range as F-D PAS saturation (19). The peak time delay τ_0, Fig. 13*b*, however, exhibits a more gradual saturation than the peak magnitude. If the analogy is made between the time delay of CPAS and the phase lag of F-D PAS, the tendency of τ_0 to remain unsaturated at larger values of β than the peak magnitude can be compared with a similar phenomenon involving the observed (20) variation of the phase lag with β in regions where the F-D PAS amplitude is well within saturation limits. Figure 13*b* further indicates that as the optical-absorption coefficient (and CPAS peak magnitude) decreases, τ_0 increases. This effect is consistent with the longer thermal time delay τ_β required for heat produced in the bulk of the liquid to reach the gas–liquid interface at longer optical-absorption depths μ_β. The β dependence of τ_0 is, however, more complicated than the perhaps expected β^{-2} relationship.

Figure 14 shows a comparison between the experimental CPAS signal from 100% by volume ink and theoretical calculations using our one-dimensional model of [6]. The theoretical signal exhibits $\tau_0 = 0$, as expected from an opaque sample for which τ_β is so short that both input and PAS signals are essentially synchronized. In this case, [3] becomes equivalent to the autocorrelation function, which peaks at zero time. The experimental time delay of Fig. 14 has been attributed to transfer-function limitations of the equipment. This feature is currently under further investigation. The microphone flyback feature yielding negative experimental cross correlations has not been incorporated in the theory and thus does not appear in

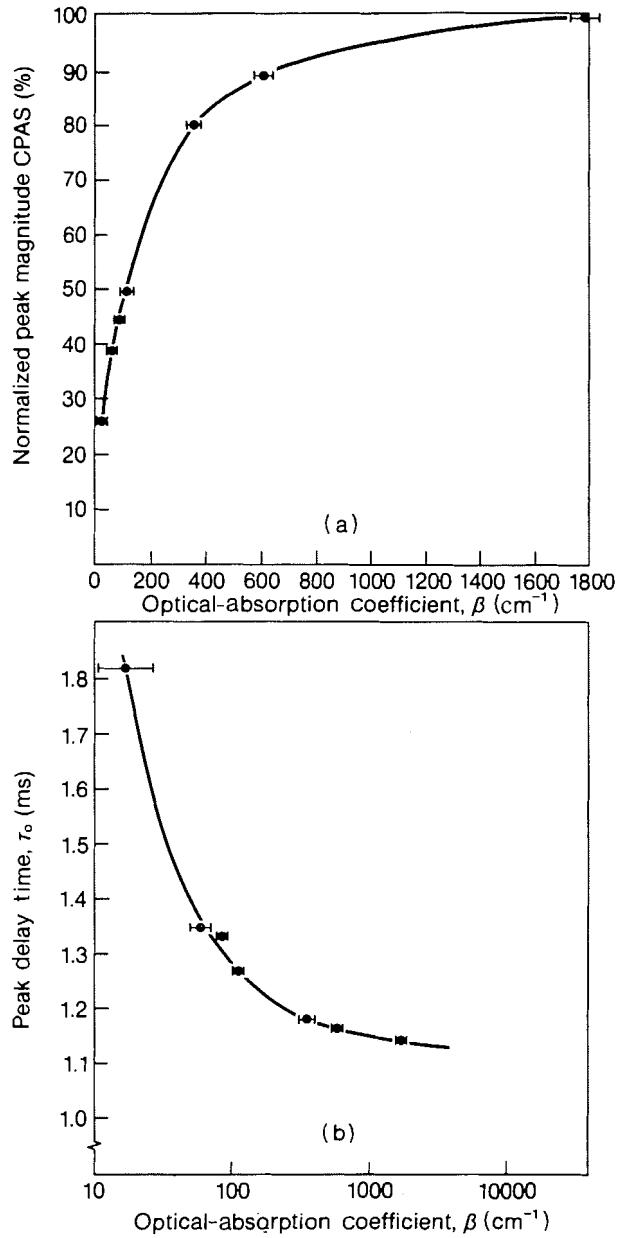

FIG. 13. Normalized CPAS signal as a function of β of aqueous ink solution; (*a*) peak magnitude; (*b*) peak time delay.

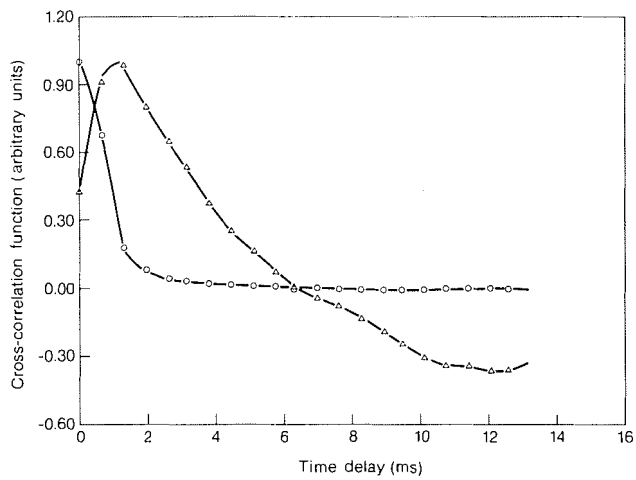

FIG. 14. Experimental (△) and theoretical (○) photoacoustic cross correlation from 100% India ink.

Fig. 14. Clearly, this figure indicates that instrumental effects have to be considered before CPAS can become quantitative as a time-delay measuring technique. The model of [4]–[9], however, is quite successful at predicting wavelength-dependent spectroscopic features quantitatively; see Figs. 6, 10, and 11.

5. Conclusions

Experimentally and theoretically, CPAS has been shown to be a photothermal technique sensitive to spectroscopic parameters in solids and liquids and capable of performing quantitative spectroscopic measurements. Our results indicate that for values of the optical-absorption coefficient above ca. $0.5\,\mathrm{cm}^{-1}$, the cross-correlation-function peak magnitude and peak time delay are related to β in ways similar to those of the amplitude and phase of F-D PAS. Our one-dimensional theoretical model exhibits parameter dependences in general agreement with the experimental evidence, with certain discrepancies presumably due to instrumental factors that were not considered in the model. It appears that the poor SNR is a limiting factor for the use of CPAS as a spectroscopic technique with transparent samples ($\beta \lesssim 5\,\mathrm{cm}^{-1}$). Photoacoustic saturation is expected to be the main limiting factor for $\beta \gtrsim 10^3\,\mathrm{cm}^{-1}$, in agreement with conventional PAS theory. The promise of CPAS to yield high SNR's at high frequencies, owing to its impulse-response equivalence and its claimed SNR superiority to pulsed time-domain PAS (3), may conceivably extend the range of high β's that can be accurately measured by photoacoustic spectroscopic techniques. The present work indicates, however, that the transducer-frequency response is a major factor limiting this range when microphone–gas coupled CPAS is employed.

Acknowledgments

The authors wish to acknowledge the financial support of the Natural Sciences and Engineering Research Council of Canada throughout this research.

1. K. KATO, S. ISHINO, and Y. SUGITANI. Chem. Lett. 783 (1980).
2. Y. SUGITANI, A. UEJIMA, and K. KATO. J. Photoacoust. **1**, 217 (1982).
3. G. F. KIRKBRIGHT, R. M. MILLER, D. E. M. SPILLANE, and I. P. VICKERY. J. Phys. (Les Ulis, Fr.), **10**, C6-243 (1983); G. F. KIRKBRIGHT, R. M. MILLER, and A. RZADKIEWICZ. J. Phys. (Les Ulis, Fr.), **10**, C6-249 (1983); G. F. KIRKBRIGHT and R. M. MILLER. Anal. Chem. **55**, 502 (1983).
4. G. F. KIRKBRIGHT, R. M. MILLER, D. E. M. SPILLANE, and Y. SUGITANI. Anal. Chem. **56**, 2043 (1984); G. F. KIRKBRIGHT, R. M. MILLER, D. E. M. SPILLANE, and I. P. VICKERY. Analyst (London), **109**, 1443 (1984).
5. A. UEJIMA, Y. SUGITANI, and K. NAGASHIMA. Anal. Sci. **1**, 5 (1985).
6. A. ROSENCWAIG and A. GERSHO. J. Appl. Phys. **47**, 64 (1976).
7. A. MANDELIS and B. S. H. ROYCE. J. Appl. Phys. **51**, 610 (1980).
8. A. MANDELIS and B. S. H. ROYCE. J. Appl. Phys. **50**, 4330 (1979).
9. J. R. SCHOONOVER, Y-L. LEE, S. N. SU, S. H. LIN, and L. EYRING. Appl. Spectrosc. **38**, 154 (1984).
10. A. MANDELIS and J. T. DODGSON. J. Phys. C, **19**, 2329 (1986).
11. A. MANDELIS, E. SIU, and S. HO. Appl. Phys. A, **33**, 153 (1984).
12. M. J. ADAMS and G. F. KIRKBRIGHT. Analyst (London), **102**, 281 (1977); **102**, 678 (1977).
13. M. J. ADAMS and G. F. KIRKBRIGHT. Spectrosc. Lett. **9**, 255 (1976).
14. A. MANDELIS, Y. C. TENG, and B. S. H. ROYCE. J. Appl. Phys. **51**, 610 (1980).
15. L. GEMLIN. *In* Handbuch der Anorganischen Chemie. Vol. 39. Springer-Verlag, Heidelberg, Federal Republic of Germany. 1974. p. 141.
16. K. D. CARLSON and D. HODUL. J. Photoacoust. **1**, 291 (1982).
17. M. F. COX and G. N. COLEMAN. Anal. Chem. **53**, 2034 (1981).
18. A. ROSENCWAIG. Adv. Electron. Electron Phys. **46**, 207 (1978).
19. J. F. MCCLELLAND and R. N. KNISELEY. Appl. Phys. Lett. **28**, 467 (1976).
20. J. C. ROARK, R. A. PALMER, and J. S. HUTCHISON. Chem. Phys. Lett. **60**, 112 (1978).